

MET.0.11 TECHNICAL NOTE NO.83

STABILITY AND PHASE SPEED ERRORS  
OF SOME FINITE DIFFERENCE SCHEMES

by

DAVID A. FORRESTER

N.B. This paper has not been published. Permission to quote from it must be obtained from the Assistant Director of the above Meteorological Branch.

APRIL 1977.

FH3<sup>B</sup>

STABILITY AND PHASE SPEED ERRORS  
OF SOME FINITE DIFFERENCE SCHEMES

1. INTRODUCTION

A theoretical analysis has been made of the stability criteria and the phase speed errors of certain finite difference schemes as applied to the one-dimensional linearised shallow water equations on both unstaggered and staggered grids. The corresponding results for the advection equation and the gravity wave equations are also derived.

The schemes considered are the Leapfrog scheme (both explicit and implicit) and the Lax-Wendroff scheme.

The results are displayed in graphical form, thus providing an easy comparison of the schemes on the different grids.

2. EQUATIONS AND GRIDS

The equations considered are :-

Case (A) - the single advection equation

$$d_t + U d_x = 0$$

Case (G) - the coupled gravity wave equations

$$\phi_t + \frac{c^2}{g} u_x = 0$$

$$u_t + g \phi_x = 0$$

Case (SW) - the shallow water equations

$$\phi_t + U \phi_x + \frac{c^2}{g} u_x = 0$$

$$u_t + U u_x + g \phi_x = 0$$

The grids considered are shown in fig.(1) in case (A) and fig.(2) in cases (G) and (SW). Grids will be referred to according to whether they are staggered or unstaggered in space and time, e.g.  $S_S U_T$  means "staggered in space, unstaggered in time".

The time levels are denoted  $\tau-1, \tau, \tau+1$  for the leap frog scheme, and  $\tau, \tau+1/2, \tau+1$  for the Lax-Wendroff scheme.

### 3. FINITE FOURIER SERIES, STABILITY CRITERION AND PHASE SPEEDS

The error analysis will be done using the method of finite fourier series. Assume that variables can be expanded as

$$d(x, t) = \sum_n d_n(t) e^{i n j \delta x}$$

with 
$$d_n(t) = \omega^\tau d_0 = |\omega|^\tau d_0 e^{i \theta \tau \delta t}$$

where  $t = \tau \delta t$ ,  $x = j \delta x$ ,  $n$  is the wave number ( $2\pi/n$  is the wavelength),  $\omega = |\omega| e^{i \theta \delta t}$  is the (complex) amplification factor and  $c' = -\theta/n$  is the phase speed of the wave solution of the finite difference equation.

The quantity  $n \delta x$  is restricted to the interval  $0$  to  $\pi$ .  $n \delta x = 2\pi/m$  corresponds to an  $m$  grid length wave.

From the expression for the amplification factor ( $\omega$ ), the stability criterion is obtained immediately from the condition  $|\omega| \leq 1$  and the phase speed

$c' = -\frac{\theta}{n} = -\frac{\theta \delta t}{n \delta t}$  is obtained by solving for  $\theta \delta t$  the pair of equations

$$\cos(\theta \delta t) = \frac{\text{Re}(\omega)}{|\omega|}$$

$$\sin(\theta \delta t) = \frac{\text{Im}(\omega)}{|\omega|}$$

3.1

$\text{Re}(\omega)$  and  $\text{Im}(\omega)$  are the real and imaginary parts of  $\omega$  respectively. Care must be taken to solve both of the above equations so as to obtain the correct phase.

The graphs which follow display against  $n\delta x$  the ratio of the phase speed of the finite difference wave to the phase speed of the exact wave solution of the differential equation which is  $U, c, U+c$  in cases (A), (G), (SW) respectively. Graphs of  $|\omega|$  against  $n\delta x$  are also included. The exact solution of the differential equation has  $|\omega| = 1$  so  $|\omega| < 1$  indicates damping and  $|\omega| > 1$  amplification.

#### 4. FINITE DIFFERENCE SCHEMES

For the simple equation

$$\frac{\partial d(x,t)}{\partial t} = F(x,t)$$

the finite difference representations are :-

(1)(a) Leapfrog (explicit)

$$\frac{1}{2\delta t} (d_{r+1} - d_{r-1}) = F_r$$

(1)(b) Leapfrog (implicit)

$$\frac{1}{2\delta t} (d_{r+1} - d_{r-1}) = \frac{1}{2} (F_{r+1} + F_{r-1})$$

(2) Lax-Wendroff

$$\frac{1}{2\delta t} (d_{r+h} - d_r) = F_r$$

$$\frac{1}{\delta t} (d_{r+1} - d_r) = F_{r+h}$$

The amplification factor is obtained directly in the Lax-Wendroff case and by solving a quadratic equation in the leapfrog case.

The advection equation and, on grids which are unstaggered in space, the gravity wave equations and the shallow water equations all give rise to the same expression for  $\omega$  (with a wave speed of  $U, c, U+c$  respectively). In the cases (G) and (SW) there are a pair of equations to solve so there are twice as many roots as in case (A) - the extra roots being obtained by replacing  $c$  by  $-c$ .

4.1(a) LEAPFROG (EXPLICIT)

In case (SW) one readily obtains the expression for the amplification

factor 
$$\omega = -i\lambda \pm \sqrt{1 - \lambda^2} \tag{4.1}$$

(+ for the physical mode, - for the computational mode)

where  $\lambda$  is given by :-

$$U_S U_T \quad \lambda = \frac{\delta t}{\delta x} (U + c) \sin(n \delta x)$$

$$S_S U_T \quad \lambda = \frac{\delta t}{\delta x} \left[ U \sin(n \delta x) + 2c \sin\left(\frac{1}{2} n \delta x\right) \right]$$

$$U_S S_T \quad \lambda = \frac{\delta t}{\delta x} (2U + 2c) \sin\left(\frac{1}{2} n \delta x\right)$$

$$S_S S_T \quad \lambda = \frac{\delta t}{\delta x} \left[ 2U \sin\left(\frac{1}{2} n \delta x\right) + c \sin(n \delta x) \right]$$

Thus  $|\omega| = 1$  if  $\lambda^2 \leq 1$

and  $|\omega| > 1$  if  $\lambda^2 > 1$

The computational mode and the physical mode have the same values of  $|\omega|$  and have phases  $\theta_c$  and  $\theta_p$  related by  $\theta_c = \pi - \theta_p$ . It is often remarked in the literature that the computational mode moves with the same speed as the physical mode but in the opposite direction and with a change of sign of the amplitude every time -step.

If the condition  $\lambda^2 \leq 1$  is satisfied with  $c > 0$ , then it is also satisfied with  $c$  replaced by  $-c$ . So if the  $U+c$  wave is stable then the  $U-c$  wave is also stable.

Graphs 1, 2, 3, 4 show plots of

$$\frac{c'}{U+c} = \frac{1}{n \delta x} \frac{\sin^{-1}(\lambda)}{(U+c) \frac{\delta t}{\delta x}}$$

against  $n \delta x$  for various values of the parameter  $\alpha$  where  $\alpha = (U+c) \frac{\delta t}{\delta x}$  for graphs 1, 2 and  $\alpha = c \frac{\delta t}{\delta x}$  for graphs 3, 4.

The value of  $\sin^{-1}(\lambda)$  is obtained by solving the simultaneous equations 3.1, and is not necessarily the same as the "principal value" of the inverse trigonometric function.

For the cases  $S_S U_T$  and  $S_S S_T$  the graphs depend on the quantity  $U/c$  and two values are chosen as being of special interest -  $U/c = 1/3$  (e.g.  $U = 100\text{ms}^{-1}$ ,  $c = 300\text{ms}^{-1}$ ) and  $U/c = 2$  (e.g.  $U = 100\text{ms}^{-1}$ ,  $c = 50\text{ms}^{-1}$ ). (In the 10 - level model, the external and second internal gravity wave speeds are about  $300\text{ms}^{-1}$  and  $50\text{ms}^{-1}$  respectively.)

For the cases  $U_S U_T$  and  $U_S S_T$ , however, the graphs are independent of  $U/c$  and it turns out that these same graphs describe also the cases (A) and (G) provided the ordinate and the parameter  $\lambda$  are redefined to contain only  $U$  or  $c$  respectively.

In fact there are only two distinct graphs for the four possible cases (G) and these coincide with the two cases (A) viz. Graph 1 describes case (A)  $U_T$ , cases (G)  $U_S U_T$  and  $S_S S_T$  and case (SW)  $U_S U_T$ . Graph 2 describes case (A)  $S_T$ , cases (G)  $S_S U_T$  and  $U_S S_T$  and case (SW)  $U_S S_T$ .

The continuous lines represent the physical modes which are stable for all  $n\delta x$ . The dashed lines represent the physical modes which become unstable for some  $n\delta x$  (Only the stable portions are shown) The dotted lines represent the corresponding computational modes.

#### 4.1 (b) LEAPFROG (IMPLICIT)

For this scheme only cases (A) and (G) have been considered. In these cases one readily finds that

$$\omega^2 = \frac{1 - i\lambda}{1 + i\lambda}$$

where  $\lambda$  is given in case (A) by

$$U_T \quad \lambda = U \frac{\delta t}{\delta x} \sin(n\delta x)$$

and in case (G) by

$$U_S U_T \quad \lambda = c \frac{\delta t}{\delta x} \sin(n\delta x)$$

$$S_S U_T \quad \lambda = 2c \frac{\delta t}{\delta x} \sin\left(\frac{1}{2}n\delta x\right)$$

Thus  $|\omega| = 1$  always.

There is a computational mode which, like the physical mode, is unconditionally stable and the phases  $\theta_c$  and  $\theta_p$  are related by  $\theta_c = \pi + \theta_p$ .

The computational mode can be interpreted as moving with the same speed and in the same direction as the physical mode but with a change of sign of the amplitude every time step.

Graphs 5 and 6 show plots of

$$\frac{c'}{c} = \frac{1}{n \delta x} \frac{\tan^{-1}(\lambda)}{c \frac{\delta t}{\delta x}}$$

for various values of the parameter  $d = \frac{c \delta t}{\delta x}$ . (This is for case (G); for case (A) replace  $c$  by  $U$ ). The continuous lines represent the physical modes and the dotted lines the computational modes.

#### 4.2 LAX-WENDROFF

Case (A)  $U_T$  gives

$$\omega = 1 - i\lambda - \frac{1}{2}\lambda^2$$

where

$$\lambda = U \frac{\delta t}{\delta x} \sin(n \delta x)$$

so  $|\omega| > 1$  always and the scheme is unconditionally unstable. It is true generally that the Lax-Wendroff scheme is unstable if the grid is not staggered in time.

Case (A)  $S_T$ , case (G)  $U_S S_T$  and case (SW)  $U_S S_T$  give

$$\omega = 1 - 2id \sin\left(\frac{1}{2}n\delta x\right) \cos\left(\frac{1}{2}n\delta x\right) - 2 \left[ d \sin\left(\frac{1}{2}n\delta x\right) \right]^2$$

so

$$|\omega|^2 = 1 - 4d^2(1-d^2) \sin^4\left(\frac{1}{2}n\delta x\right)$$

and the scheme is stable if  $d \leq 1$

Graph 7 shows  $|\omega|$  and graph 8 shows  $c'/(U+c)$ . The dashed lines represent modes which are unstable for some (or all)  $n\delta x$ . Both the stable and unstable portions of such curves are shown.

Case (G)  $S_S S_T$  gives

$$\omega = 1 - i\alpha \sin(n\delta x) \cos(\frac{1}{2}n\delta x) - \frac{1}{2} [\alpha \sin(n\delta x)]^2$$

where  $\alpha = c \frac{\delta t}{\delta x}$

so  $|\omega|^2 = 1 - [\alpha \sin(n\delta x) \sin(\frac{1}{2}n\delta x)]^2 \{ 1 - [\alpha \cos(\frac{1}{2}n\delta x)]^2 \}$

and the scheme is stable if  $\alpha \leq 1$ . For  $\alpha > 1$  the scheme becomes unstable at long wavelengths. The results of this case are given in graphs 9 and 10.

Case (SW)  $S_S S_T$  gives

$$\omega = 1 - i\lambda \cos(\frac{1}{2}n\delta x) - \frac{1}{2}\lambda^2$$

where  $\lambda = \frac{\delta t}{\delta x} [2U \sin(\frac{1}{2}n\delta x) + c \sin(n\delta x)]$

so  $|\omega|^2 = 1 - \lambda^2 \sin^2(\frac{1}{2}n\delta x) + \frac{1}{4}\lambda^4$

and the scheme is stable provided  $\alpha \equiv c \frac{\delta t}{\delta x} \leq \frac{1}{U/c + 1}$

If  $\alpha > \frac{1}{U/c + 1}$  then instability sets in at the long waves. Graphs 11

and 12 show the results for the two cases  $U/c = 1/3$  and  $U/c = 2$ .

## 5. REMARKS

### Leapfrog (explicit)

The computational mode is stable or unstable for the same values of  $n\delta x$  as is the physical mode. In general the computational mode (when stable) moves much faster than the physical mode. For long waves the speed of the computational mode becomes infinite.

Instability sets in at  $n\delta x = \pi/2$  at  $\alpha = 1$  in the case of graph 1 and at  $n\delta x = \pi$  at  $\alpha = 1/2$  in the case of graph 2. Note that graph 2 is identical to graph 1 if truncated at  $n\delta x = \pi/2$  and  $n\delta x$  is doubled and  $\alpha$  is halved. Thus staggering effectively removes completely the 2 to 4 grid length waves.

In the cases of graphs 3 and 4, instability sets in at  $n\delta x = \pi$  at  $\alpha = 1/2$  ( $c \frac{\delta t}{\delta x} = 1/2$ ) and  $\alpha = \frac{1}{2U/c}$  ( $U \frac{\delta t}{\delta x} = 1/2$ ) respectively.

However, in both cases instability has already set in at longer wavelengths ( $n\delta x$  between  $\pi/2$  and  $\pi$ ) for smaller values of  $\alpha$ .

Considering the shallow water equations, 2 grid length waves are more accurately represented on the  $S_S U_T$  grid in the case  $U/c = 1/3$  than on the  $S_S S_T$  grid. However, the converse is true in the case  $U/c = 2$ . The 2 grid length waves are stationary on the  $U_S U_T$  grid, and most accurately represented on the  $U_S S_T$  grid.

For short wavelengths (e.g. 2 to 4 grid length waves in the case of graph 1) the choice as to which mode should be called the "physical" mode and which the "computational" mode is not altogether clear. In this report the convention is that a + sign in equation 4.1 represents a physical mode and a - sign a computational mode. In the case of  $\alpha = 1$  in graph 1 the dotted line for  $\pi/2 \leq n \delta x \leq \pi$  is an exact solution, so this should be called the physical mode. However, for  $\alpha < 1$  the choice is not so obvious.

### Leapfrog (implicit)

The implicit case is always worse than the explicit case. Indeed the best implicit case (small  $\delta t$ ) is the same as the worst explicit case (small  $\delta t$ ). Increasing  $\delta t$  seriously reduces the accuracy of the phase speeds. Compare this result with the explicit case where increasing  $\delta t$  (within the limit of stability) increases the accuracy of the phase speeds.

Note again that graph 6 is identical to graph 5 truncated at  $n \delta x = \pi/2$  with  $n \delta x$  doubled and  $\alpha$  halved.

### Lax-Wendroff

On the  $U_S S_T$  grid all wavelengths become unstable simultaneously (at  $\alpha = 1$  in graph 7) whereas on the  $S_S S_T$  grid instability sets in at large wavelengths (at  $\alpha = 1$  in graph 9 and at  $\alpha = \frac{1}{U/c + 1}$  in graph 11). Compare this result with that of the Leapfrog scheme where instability sets in for wavelengths between 2 and 4 grid lengths.

The 2 grid length waves are stationary in all cases on the  $S_S S_T$  grid, and in the cases  $\alpha < 1/\sqrt{2}$  on the  $U_S S_T$  grid.

In all the explicit cases considered, the phase speed accuracy improves rapidly as the limiting value of  $\alpha$  for stability is approached. Moreover in certain cases this limiting value of  $\alpha$  gives the exact solution to the differential equation.

This is because in this limit the finite difference scheme becomes equivalent in these cases to the method of characteristics. It is thus crucial to use the longest time step compatible with linear computational stability.

Furthermore, considering for example Graph 3a, a dramatic improvement in the accuracy of the phase speeds of all waves with wavelengths greater than about 3 grid lengths, can be achieved by using the unstable value  $\alpha = 0.48$ . This "unstable" scheme will be computationally stable provided the unstable wavelengths are completely eliminated at each time step (e.g. by Fourier analysis).

These remarks are valuable when dealing with the linearised equations (where  $U$  and  $c$  are constants). However, in the 10-level model  $U$  can vary from  $0 \text{ ms}^{-1}$  to as much as  $100 \text{ ms}^{-1}$ , and  $c$  has 10 distinct values ranging from  $5 \text{ ms}^{-1}$  to  $300 \text{ ms}^{-1}$  (and each of these values is slightly varied in itself). Choice of a timestep to give the best accuracy for a fast gravity (or advection) wave will result in poor accuracy for a slow wave. As far as the gravity waves are concerned it would be much better to use a larger timestep for the slow waves and a smaller timestep for the fast waves thus keeping the best value of  $\alpha$  for all waves.

For small values of  $\alpha$ , the phase speed  $c'$  is almost independent of  $\alpha$  and for example in the case of the Leapfrog scheme (both explicit and implicit) on a  $U_s U_T$  grid the curves tend to the curve

$$y = \frac{\sin(n\delta x)}{n\delta x} .$$

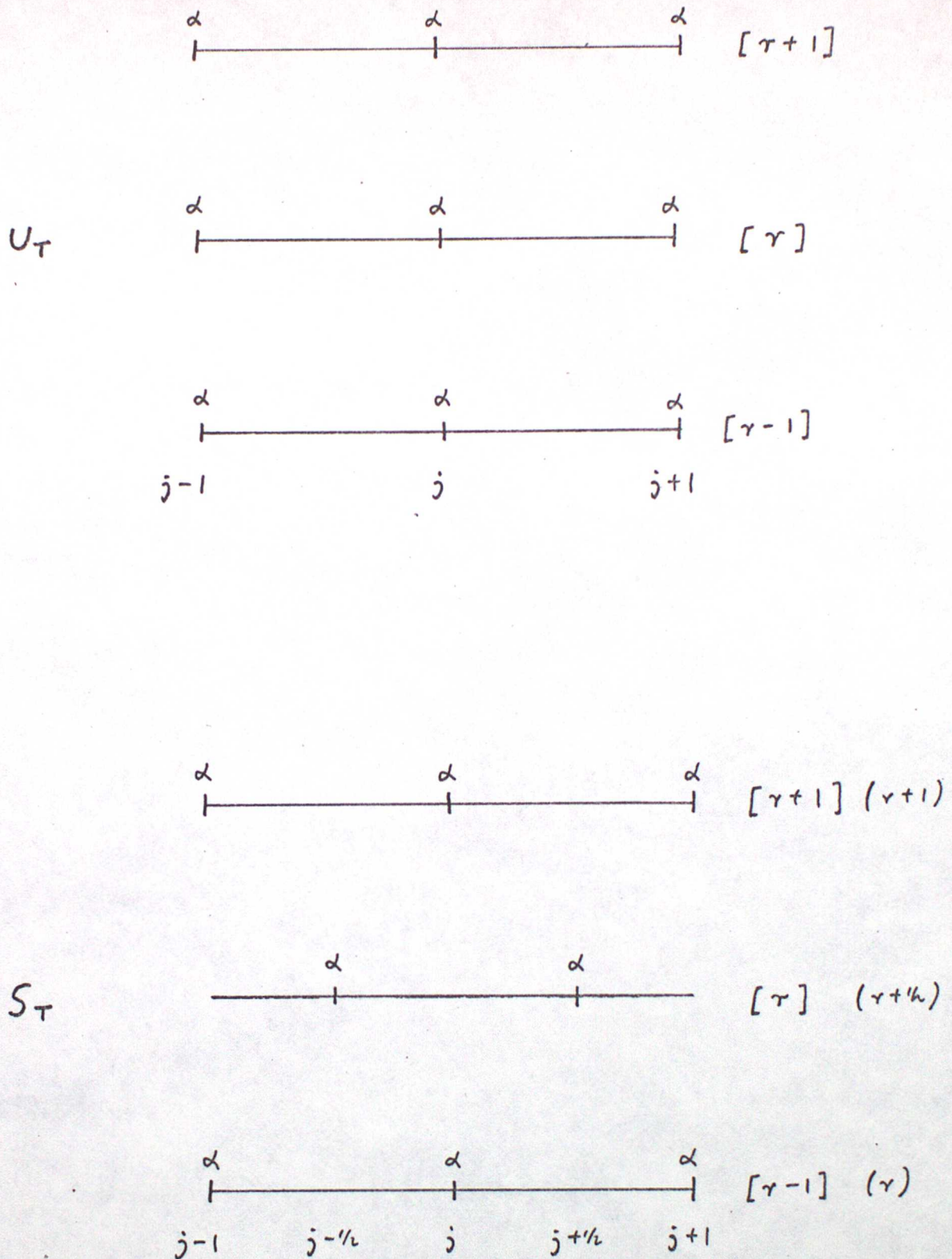


Fig.(1)

Grids used for the advection equations.

Time levels are denoted  $[ ]$  for the Leapfrog scheme, and  $( )$  for the Lax-Wendroff scheme.

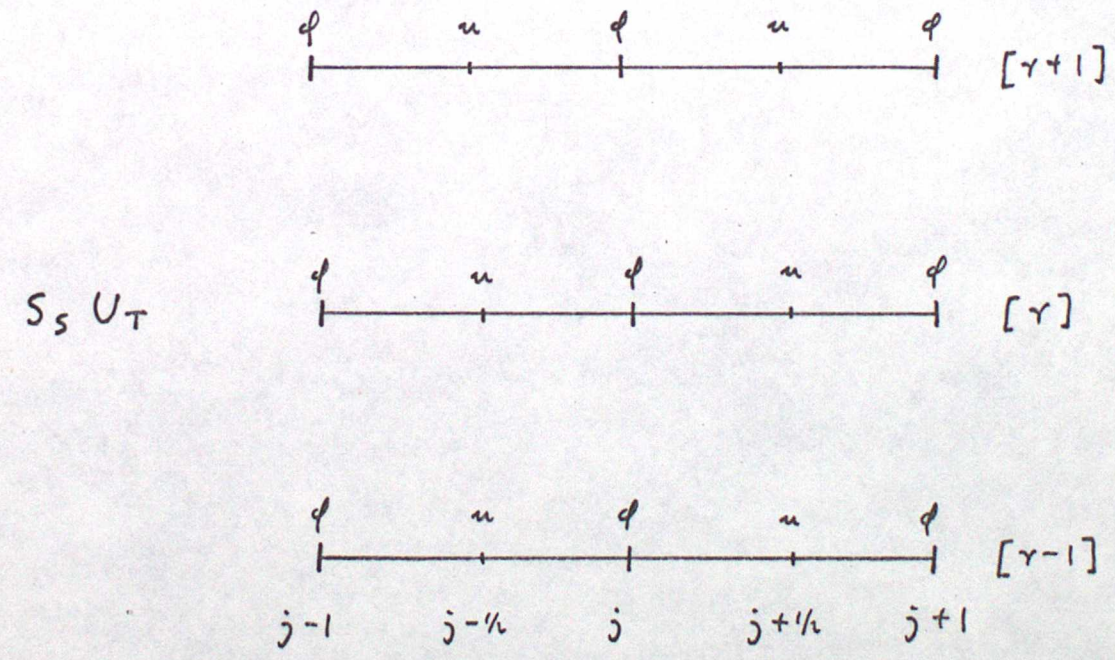
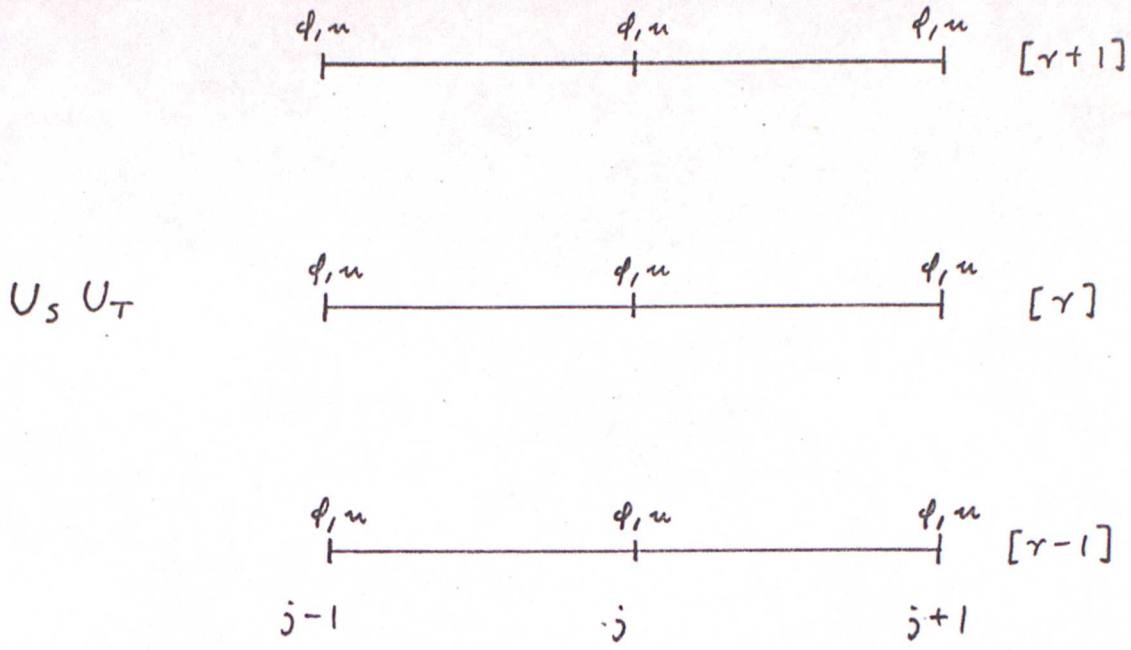
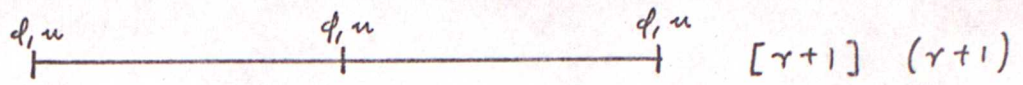
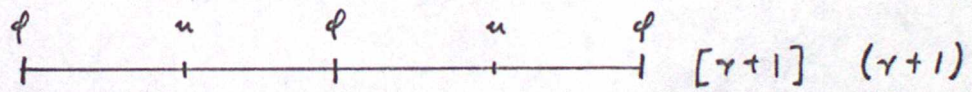
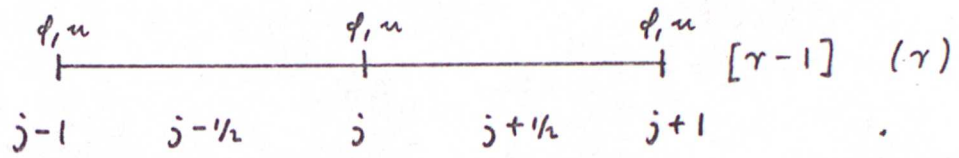
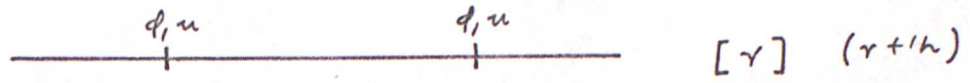


Fig (2a)

Grids used for the gravity wave and shallow water equations. Time levels are denoted [ ] for the Leapfrog scheme, and ( ) for the Lax-Wendroff scheme.



$U_S S_T$



$S_S S_T$

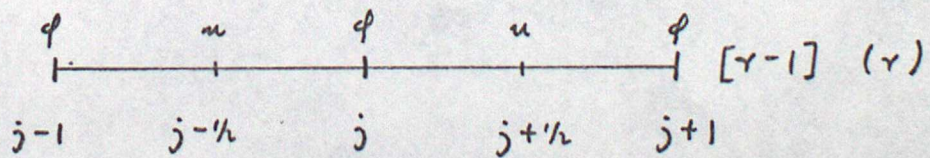
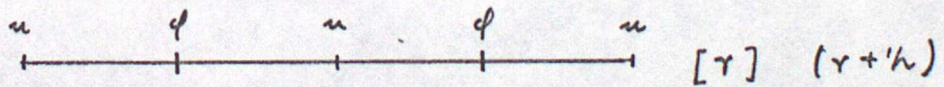


Fig (2b)

## NOTES ON GRAPHS

The following graphs display as ordinate the phase speed  $c'$  (normalised to unity for long wavelengths) for the Leapfrog and Lax-Wendroff schemes and the amplification factor  $|w|$  for the Lax-Wendroff scheme. The abscissa is  $n\delta x$ .

All curves are labelled by the value of the parameter  $\alpha$ , defined below each graph.

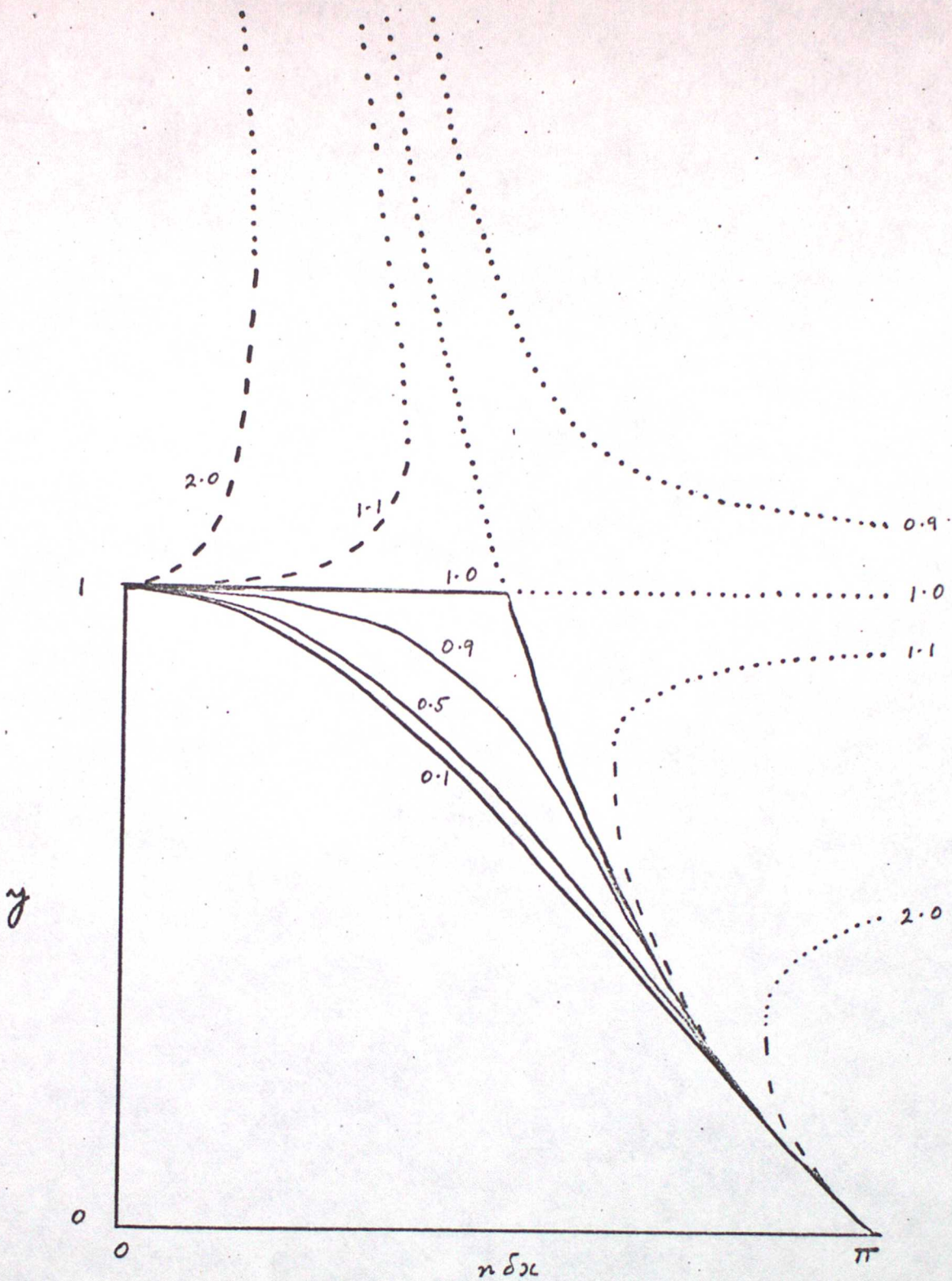
The continuous lines represent physical modes which are stable.

The dashed lines represent physical modes which are unstable for some (or all)  $n\delta x$ .

In the case of the Leapfrog scheme, only the stable portions of such curves are shown.

In the case of the Lax-Wendroff scheme both the stable and unstable portions are shown.

The dotted lines represent computational modes.

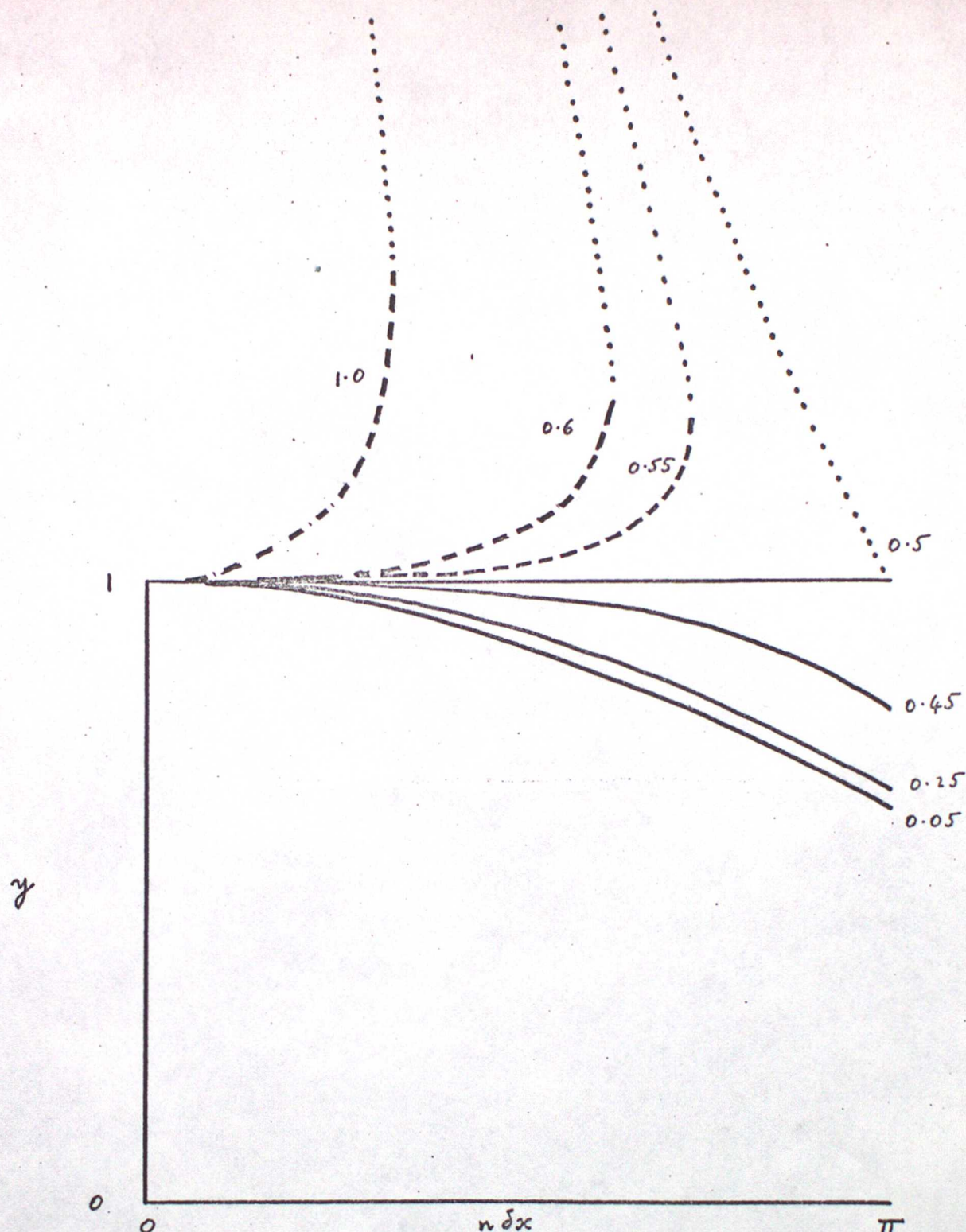


Graph 1

LEAPFROG (EXPLICIT)

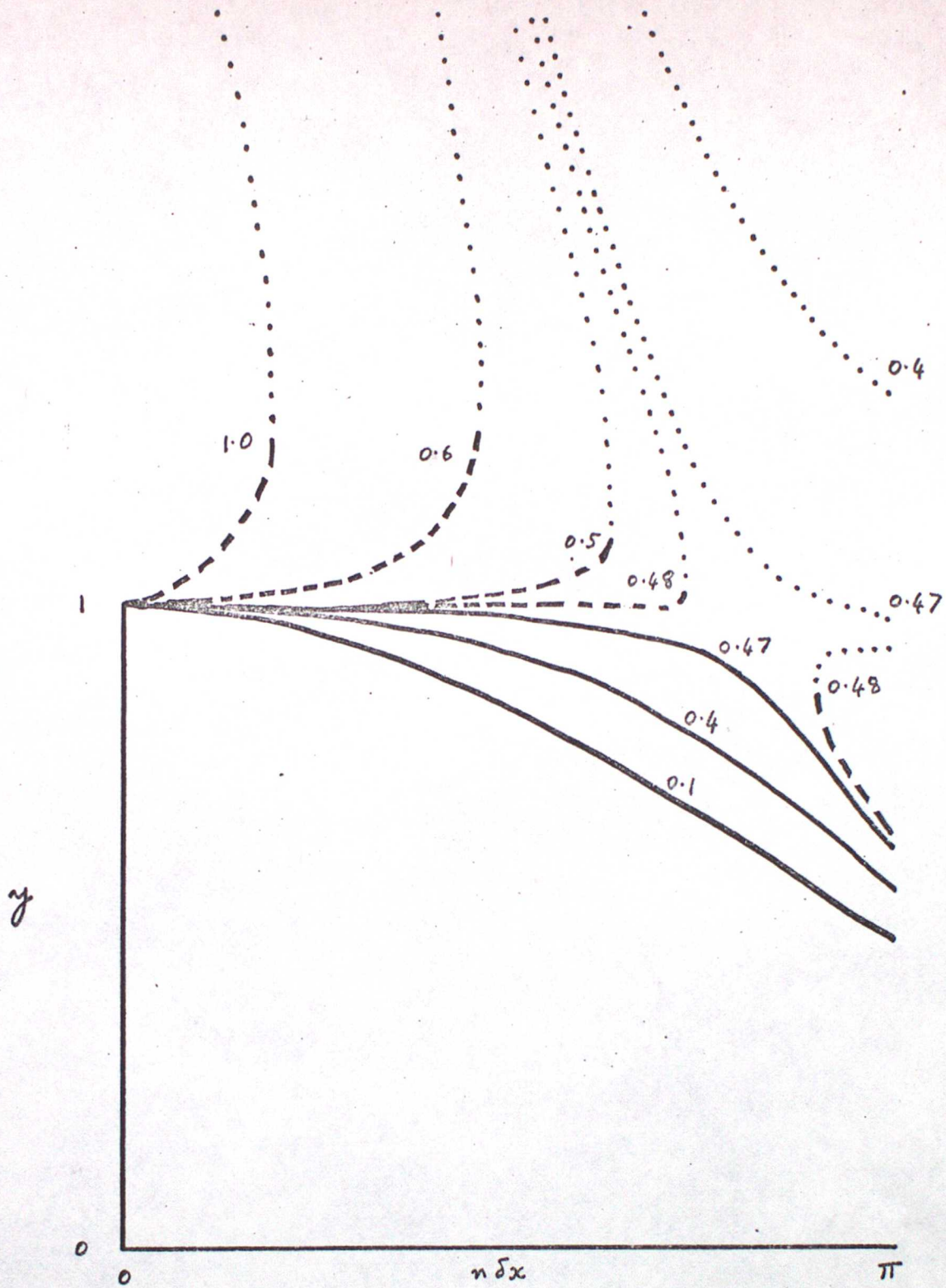
PHASE SPEED

- |      |                         |                                      |                  |
|------|-------------------------|--------------------------------------|------------------|
| (A)  | $U_T$                   | $\alpha = U \delta t / \delta x$     | $y = c' / U$     |
| (G)  | $U_S U_T$ and $S_S S_T$ | $\alpha = c \delta t / \delta x$     | $y = c' / c$     |
| (SW) | $U_S U_T$               | $\alpha = (U+c) \delta t / \delta x$ | $y = c' / (U+c)$ |



Graph 2 LEAPFROG (EXPLICIT) PHASE SPEED

- |      |                         |                                 |                |
|------|-------------------------|---------------------------------|----------------|
| (A)  | $S_T$                   | $d = U \delta t / \delta x$     | $y = c'/U$     |
| (E)  | $S_S U_T$ and $U_S S_T$ | $d = c \delta t / \delta x$     | $y = c'/c$     |
| (SW) | $U_S S_T$               | $d = (U+c) \delta t / \delta x$ | $y = c'/(U+c)$ |



Graph 3a

LEAPFROG (EXPLICIT)

PHASE SPEED

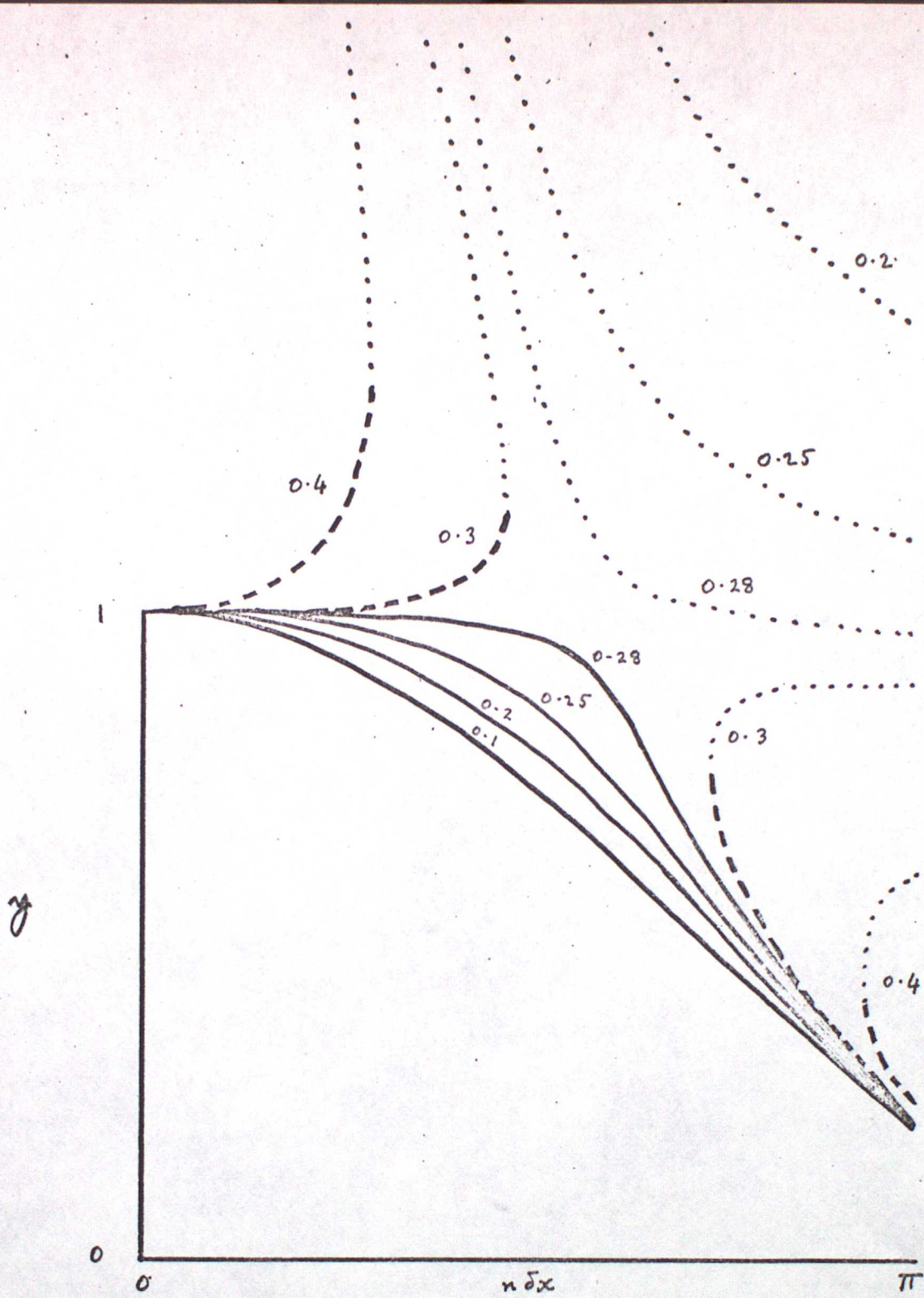
(SW)

$S_S U_T$

$U/c = 1/3$

$\alpha = c\delta t/\delta x$

$y = c'/(U+c)$

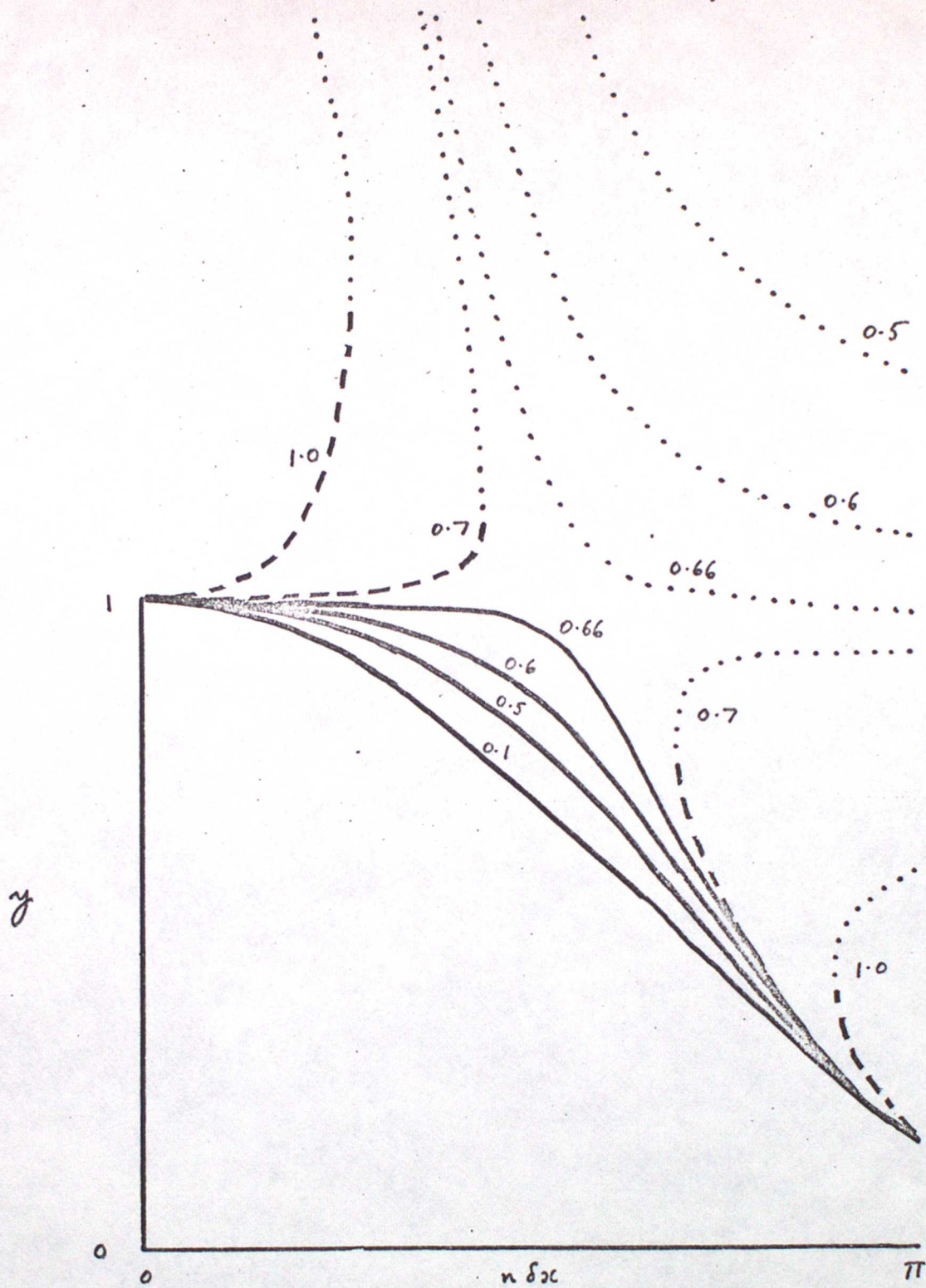


Graph 3b

LEAPFROG (EXPLICIT)

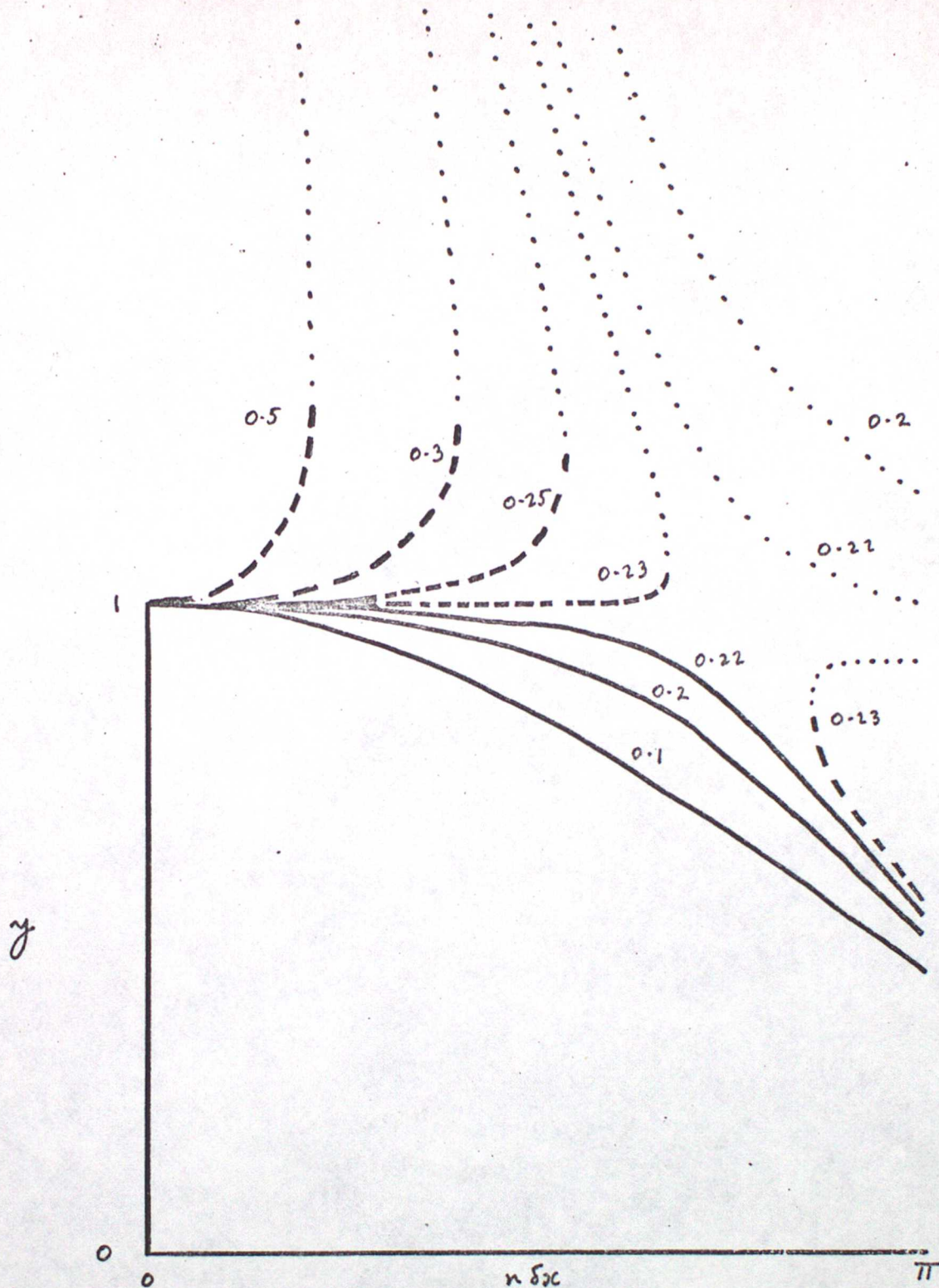
PHASE SPEED

(SW)  $S_S U_T$   $u/c = 2$   $\alpha = c\delta t / \delta x$   $\gamma = c' / (u + c)$



Graph 4a LEAPFROG (EXPLICIT) PHASE SPEED

(SW)  $S_S S_T$   $v/c = 1/3$   $\alpha = c \delta x / \delta x$   $y = c' / (v + c)$



Graph 4b

LEAPFROG (EXPLICIT)

PHASE SPEED

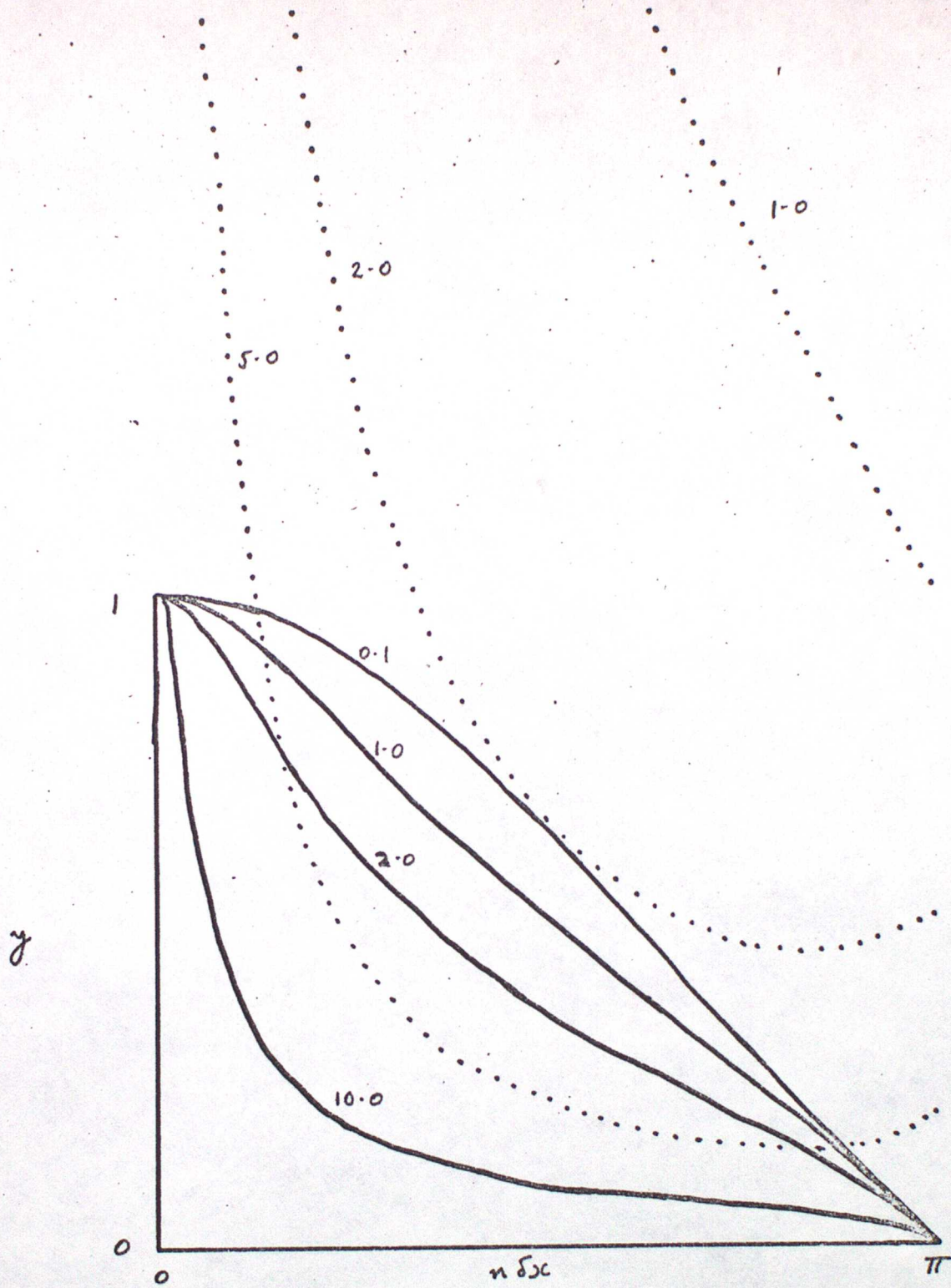
(SW)

$S_S S_T$

$U/c = 2$

$\alpha = c \delta t / \delta c$

$y = c' / (U + c)$



Graph 5

LEAPFROG (IMPLICIT)

PHASE SPEED

(A)  $U_T$

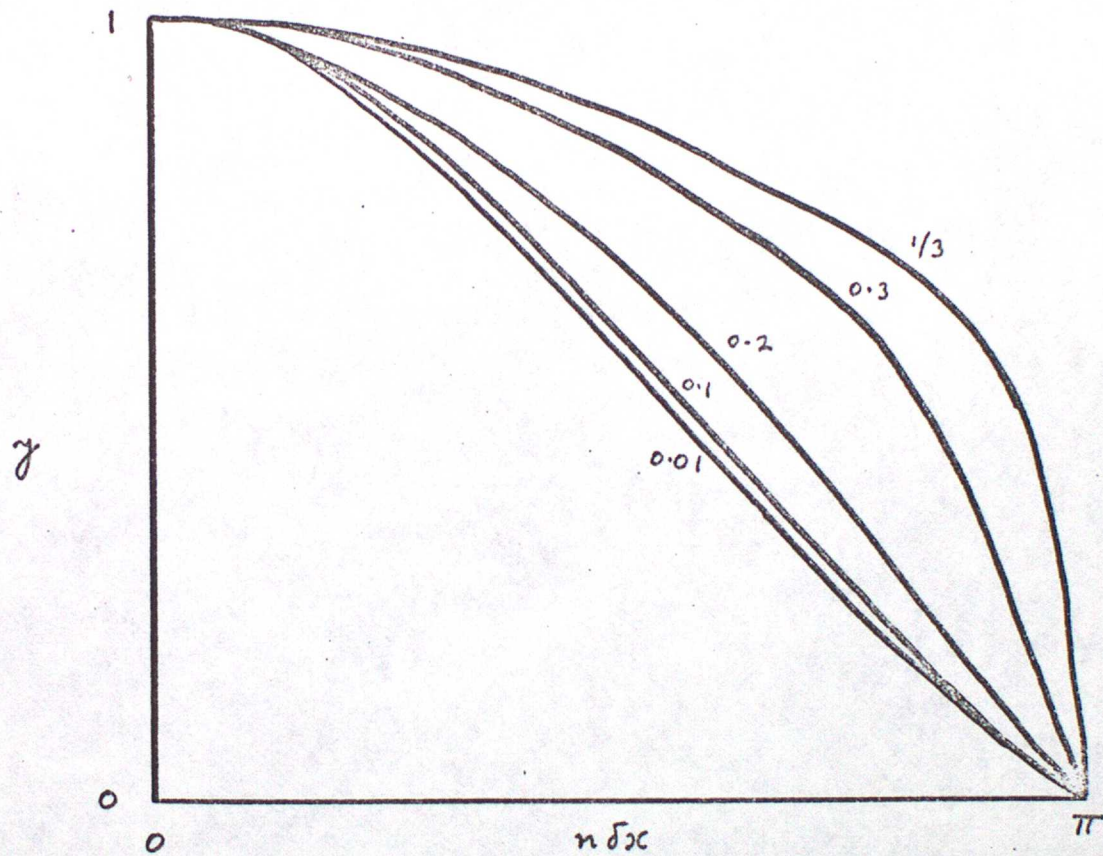
$$d = U \delta x / \delta c$$

$$\gamma = c'/U$$

(G)  $U_S U_T$

$$d = c \delta x / \delta c$$

$$\gamma = c'/c$$



Graph 12b

LAX-WENDROFF

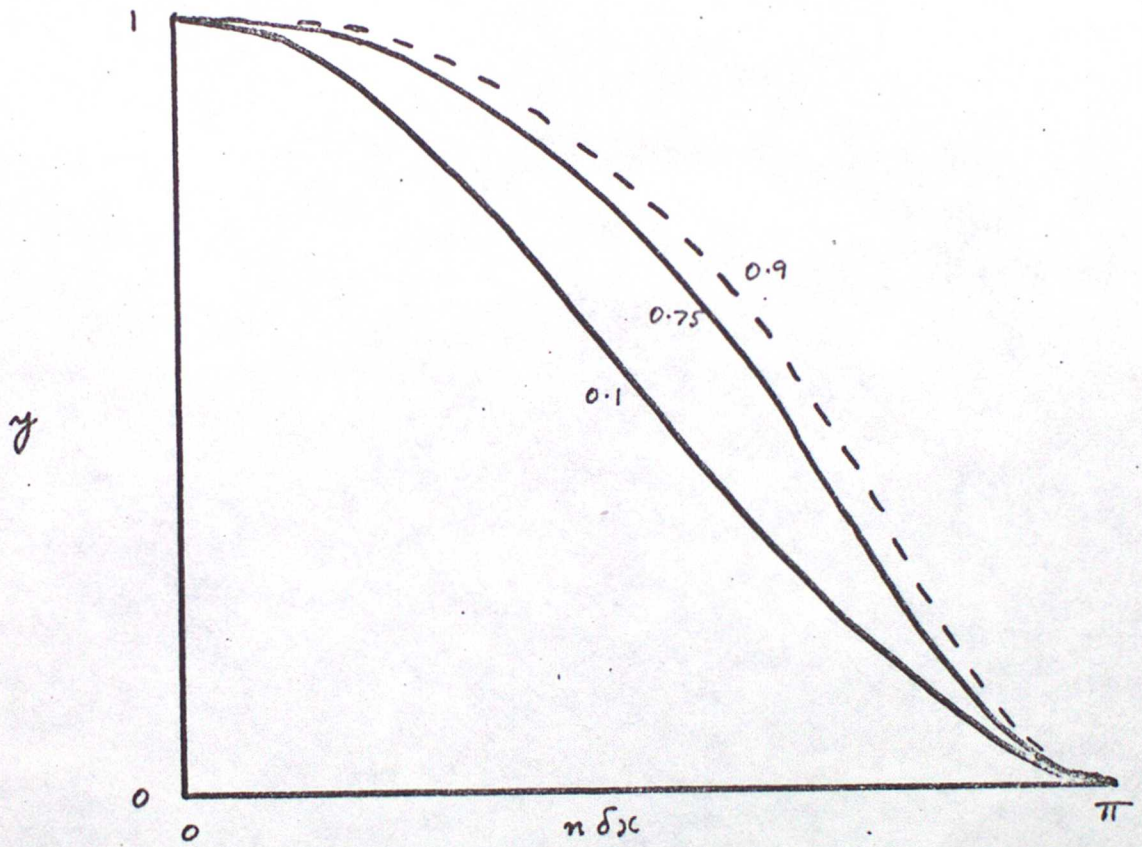
PHASE SPEED

(SW)  $S_S S_T$

$$u/c = 2$$

$$\alpha = c\delta x/\delta x$$

$$\gamma = c'/(u+c)$$

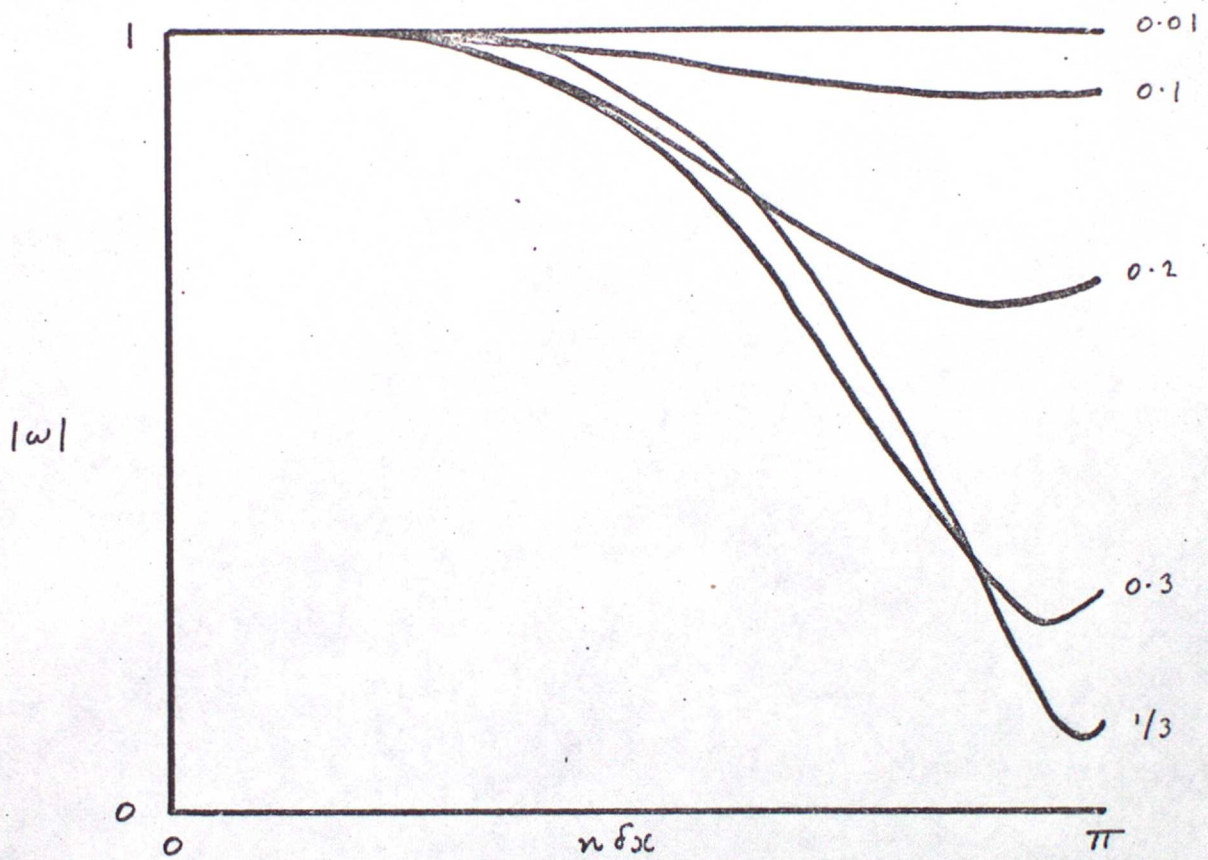


Graph 12a

LAX-WENDROFF

PHASE SPEED

(sw)  $S_S S_T$   $u/c = 1/3$   $d = c\delta t/\delta x$   $\gamma = c'/(u+c)$

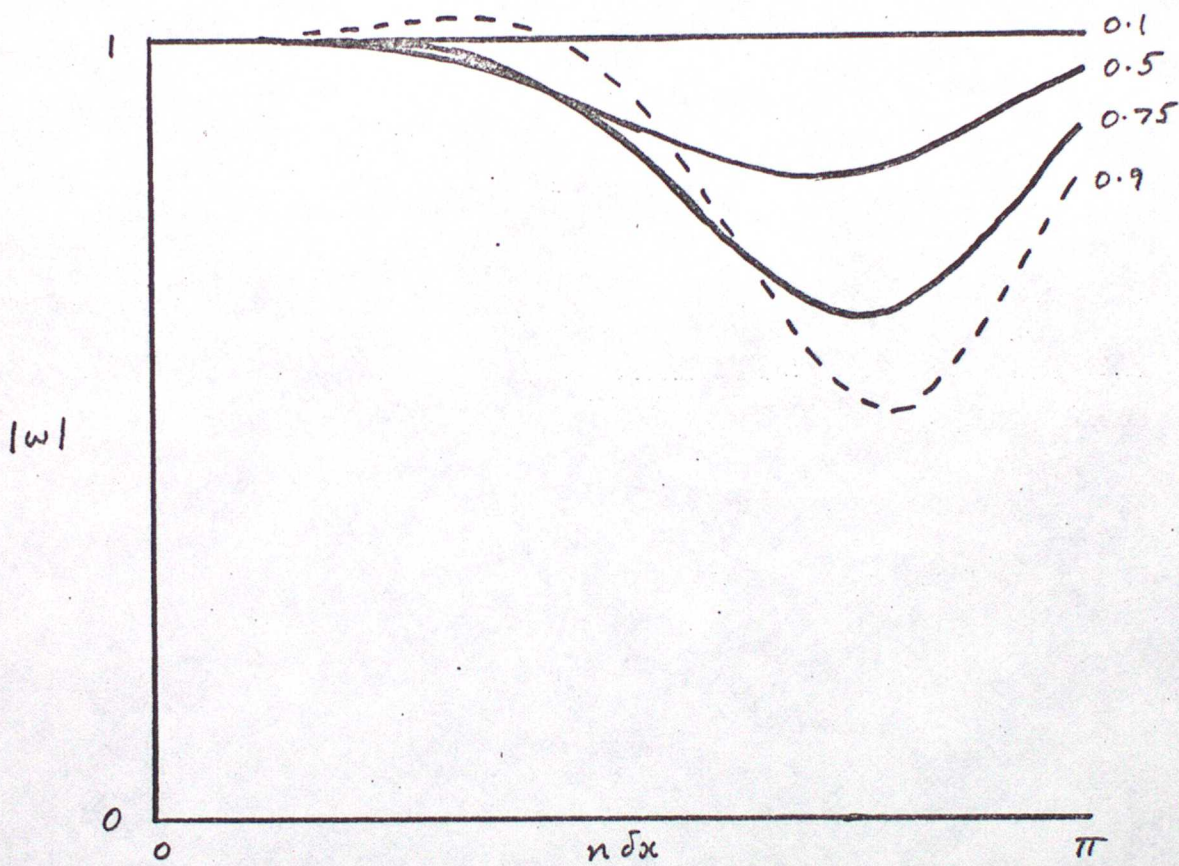


Graph 11b

LAX-WENDROFF

AMPLIFICATION FACTOR

(sw)  $S_S S_T$   $v/c = 2$   $\alpha = c \delta t / \delta x$



Graph 11a

LAX-WENDROFF

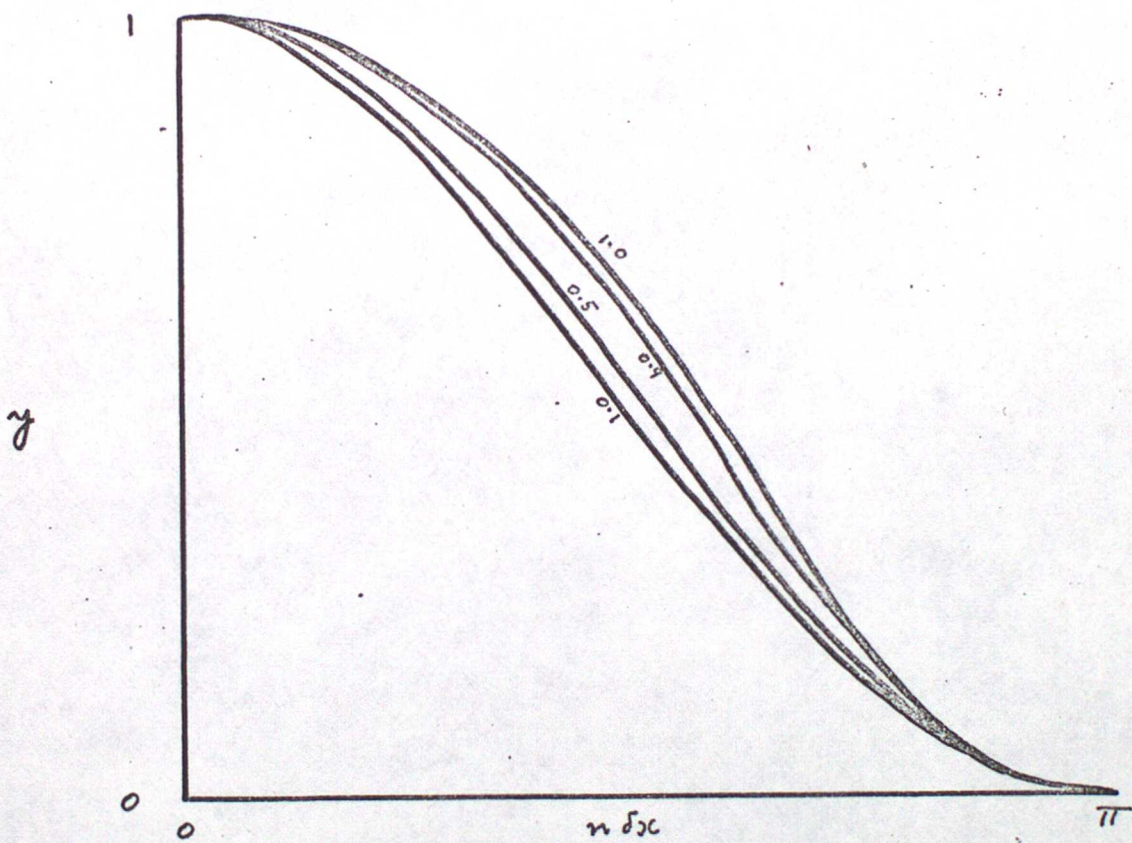
AMPLIFICATION FACTOR

(sw)

$S_S S_T$

$$u/c = 1/3$$

$$\alpha = c\delta t/\delta x$$



Graph 10

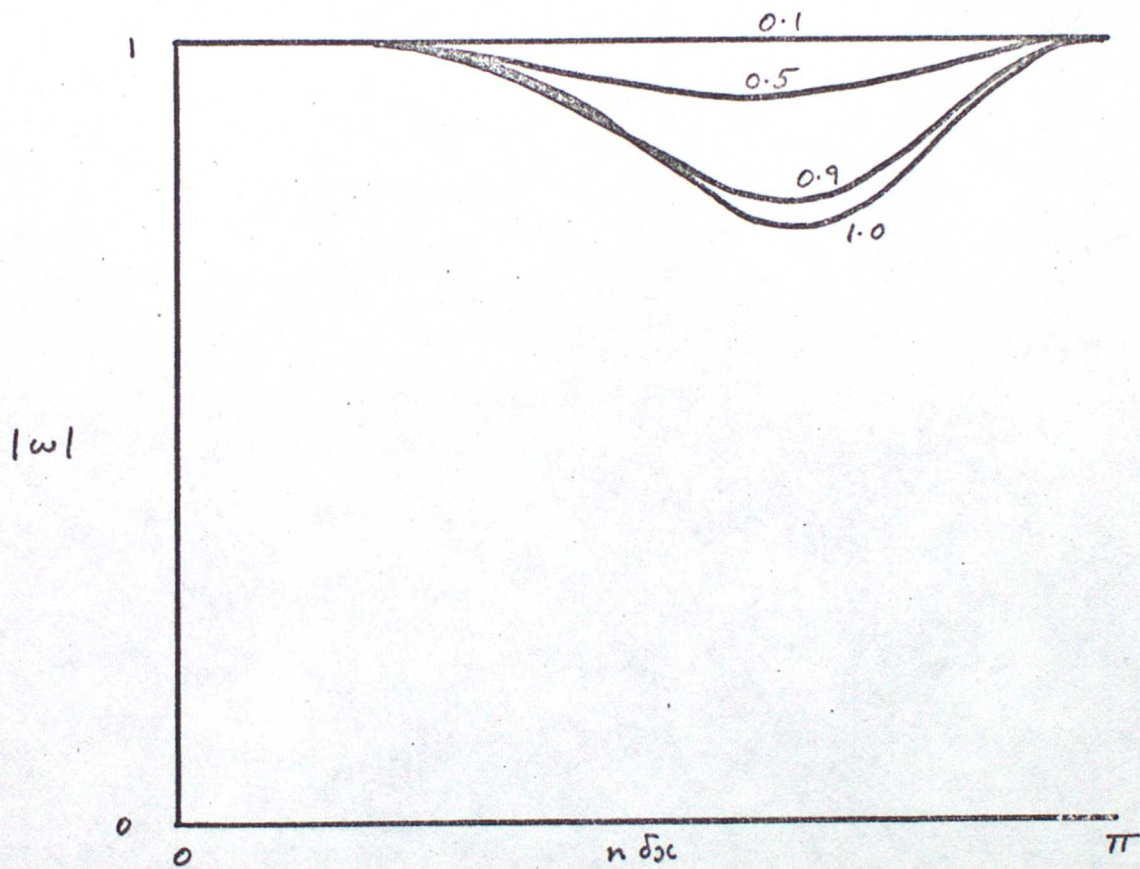
LAX-WENDROFF

PHASE SPEED

(G)  $S_S S_T$

$\alpha = c\delta x / \delta c$

$\gamma = c'/c$



Graph 9

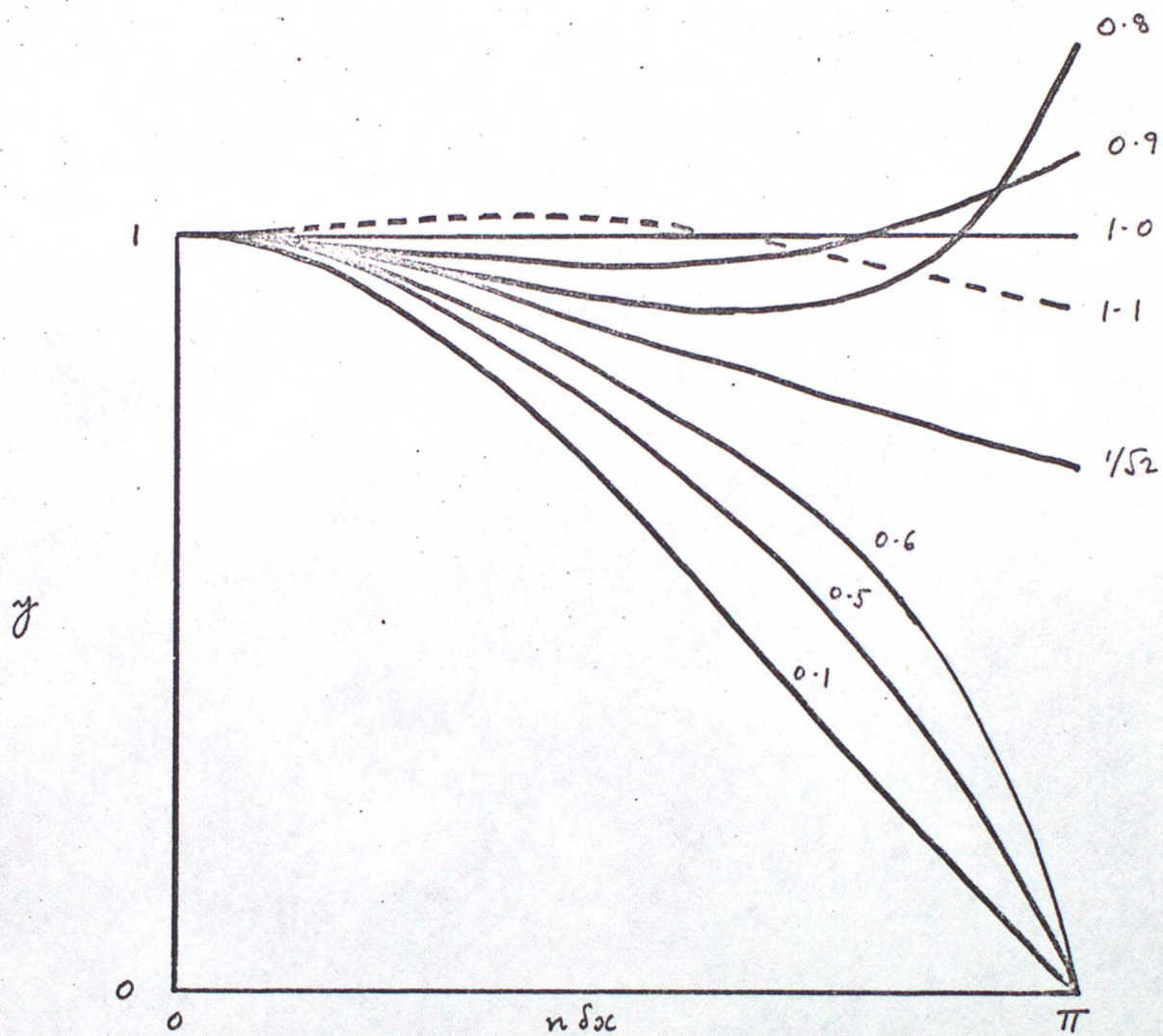
LAX-WENDROFF

AMPLIFICATION FACTOR

(G)

$S_S S_T$

$$\alpha = c \delta x / \delta x$$



Graph 8

LAX-WENDROFF

PHASE SPEED

(A)  $S_T$

$$\alpha = U \delta t / \delta x$$

$$\gamma = c' / U$$

(G)  $U_S S_T$

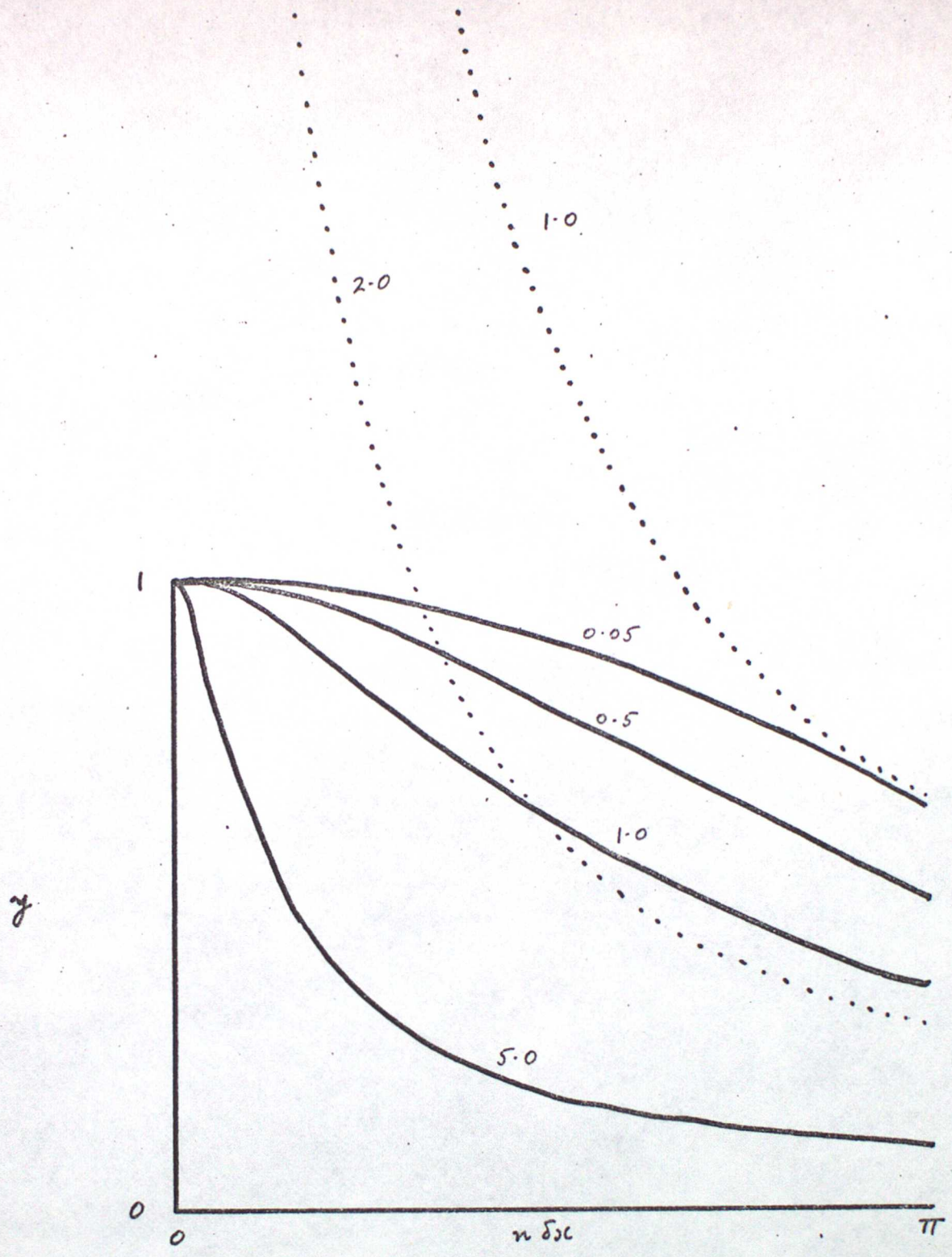
$$\alpha = c \delta t / \delta x$$

$$\gamma = c' / c$$

(SW)  $U_S S_T$

$$\alpha = (U + c) \delta t / \delta x$$

$$\gamma = c' / (U + c)$$



Graph 6

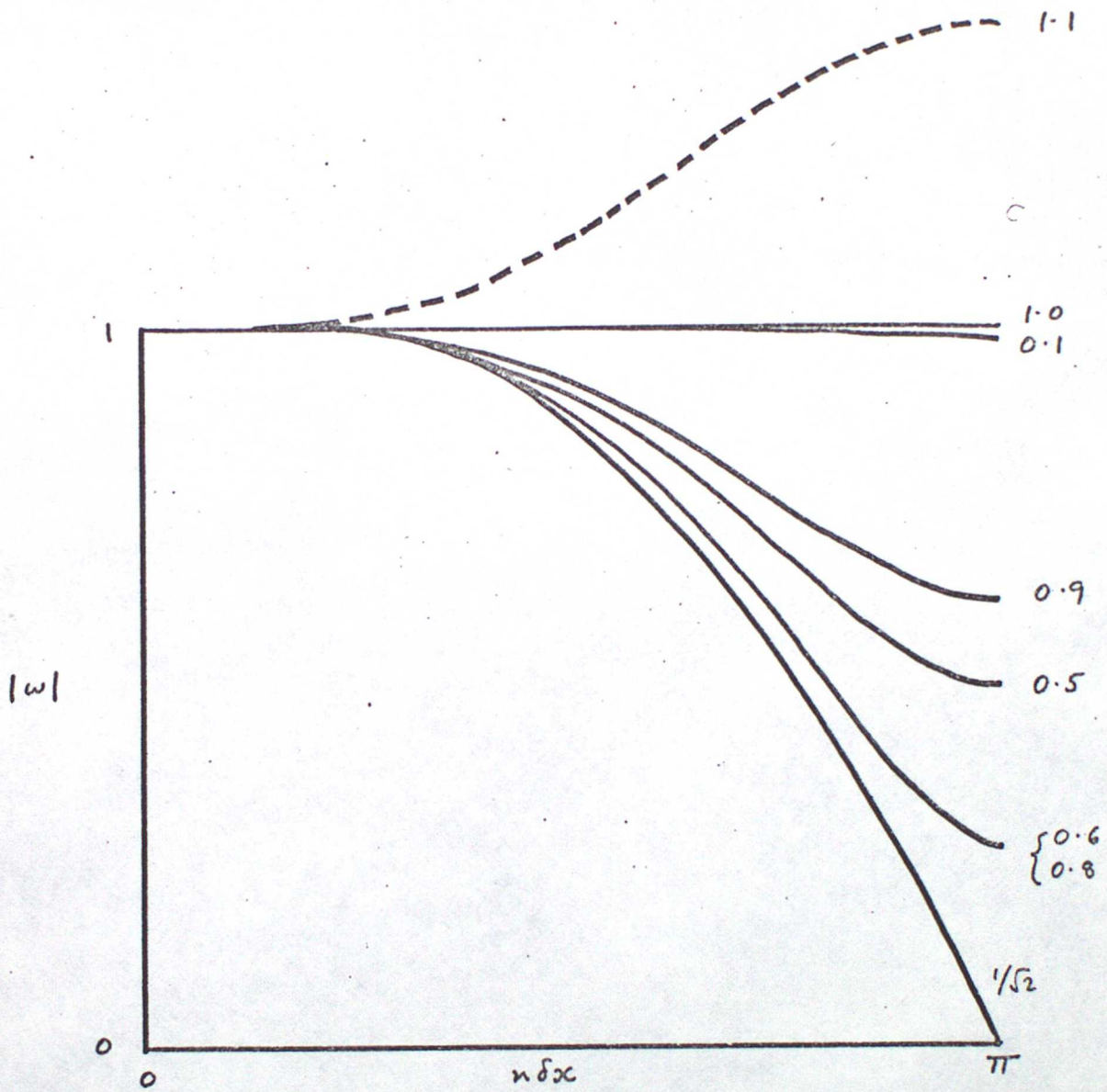
LEAPFROG (IMPLICIT)

PHASE SPEED

(c)  $S_S U_T$

$\alpha = c \delta x / \delta x$

$\gamma = c'/c$



Graph 7

LAX-WENDROFF

AMPLIFICATION FACTOR

(A)  $S_T$   $\alpha = U \delta t / \delta x$

(G)  $U_S S_T$   $\alpha = c \delta t / \delta x$

(sw)  $U_S S_T$   $\alpha = (U+c) \delta t / \delta x$